

Late-time evolution of the Universe within a two-scalar-field cosmological model

Paulo M. Sá*

*Departamento de Física, Faculdade de Ciências e Tecnologia,
Universidade do Algarve, Campus de Gambelas, 8005-139 Faro, Portugal*

(Dated: March 2, 2021)

We investigate the late-time evolution of the Universe within a cosmological model in which dark matter and dark energy are identified with two interacting scalar fields. Using methods of qualitative analysis of dynamical systems, we identify all cosmological solutions of this model. We show that viable solutions—in the sense that they correspond to a cosmic evolution in which a long enough matter-dominated era is followed by a current era of accelerated expansion—can be found in several regions of the parameter space. These solutions can be divided into two categories, namely, solutions that evolve to a state of everlasting accelerated expansion, in which the energy density of the dark-matter field rapidly approaches zero and the evolution becomes entirely dominated by the dark-energy field, and solutions in which the stage of accelerated expansion is temporary and the ratio between the energy densities of dark energy and dark matter tends, asymptotically, to a constant nonzero value.

I. INTRODUCTION

One of the most striking developments of modern cosmology was the discovery that the Universe is presently undergoing a period of accelerated expansion [1, 2], driven by a still unknown form of energy, called dark energy, which accounts for about 69% of the total energy density of the Universe [3].

The simplest candidate for dark energy is the cosmological constant, whose energy density remains unchanged throughout the evolution of the Universe. Although consistent with current observational data, the cosmological constant is unsatisfactory from the theoretical point of view, since its energy scale estimated at both the classical and quantum levels strongly deviates from the value required by cosmic observations [4, 5].

An alternative and appealing approach is to consider the role of dark energy to be played, not by a cosmological constant, but rather by a dynamical scalar field, whose potential energy starts to dominate the evolution of the Universe at later times, giving rise to a period of cosmic acceleration, in a way similar to primordial inflation (for a review on dynamical dark energy see Ref. [6]).

A natural extension of this dynamical approach is to consider that dark matter—whose physical nature, after decades of intense experimental efforts, still remains unknown [7]—can also be identified with a scalar field. This field could then, under certain circumstances, become the dominant component of the Universe, giving rise to a matter-dominated era of evolution needed for structure formation.

Identifying both dark energy and dark matter with scalar fields opens the possibility to unify two seemingly disparate phenomena under the same theoretical framework. This unifying effort can be taken even further if one of the scalar fields also plays the role of the inflaton

in the early Universe (for such triple unifications see, for instance, Refs. [8–17]).

In a recent article [15], a unified description of inflation, dark energy, and dark matter was proposed within a two-scalar-field cosmological model given by the action¹

$$S = \int d^4x \sqrt{-g} \left[\frac{R}{2\kappa^2} - \frac{1}{2}(\nabla\phi)^2 - \frac{1}{2}e^{-\alpha\kappa\phi}(\nabla\xi)^2 - e^{-\beta\kappa\phi}V(\xi) \right], \quad (1)$$

where α and β are dimensionless parameters. Such an action arises in a great variety of gravity theories, like the Jordan-Brans-Dicke theory, Kaluza-Klein theories, $f(R)$ -gravity, and string theories (see Ref. [18, 19] for a derivation of the above action within these theories), as well as the hybrid metric-Palatini theory [20, 21]. According to the proposed unification scenario, for an appropriate choice of the potential $V(\xi)$ (see below), inflation, assumed to be of the warm type, is driven by the scalar field ξ , which shortly after the end of the inflationary period decouples from radiation and starts behaving like a cold-dark-matter fluid; after a radiation-dominated era, which encompasses the primordial nucleosynthesis period, the dark-matter fluid, together with ordinary baryonic matter, gives rise to a matter-dominated era, long enough to allow for structure formation; finally, at recent times, the second scalar field ϕ emerges as the dominant component of the Universe, giving rise to an era of accelerated expansion. Resorting to numerical simulations, it was shown in Ref. [15] that, for certain values of the parameters α and β , the picture emerging in this unified description of inflation, dark energy, and dark matter is consistent with the standard cosmological model.

¹ We adopt in this article the natural system of units and use the notation $\kappa \equiv \sqrt{8\pi G} = \sqrt{8\pi}/m_p$, where G is the gravitational constant and $m_p = 1.22 \times 10^{19}$ GeV is the Planck mass.

*Electronic address: pmsa@ualg.pt

In the present article, we further investigate the two-scalar-field cosmological model given by action (1), using the powerful methods of qualitative analysis of dynamical systems. Our goal is to perform a thorough investigation of the dynamical system arising in our model, covering the entire parameter space (α, β) , in order to identify all solutions that reproduce the later stages of evolution of the Universe, namely, the dark-matter- and dark-energy-dominated eras.

This article is organized as follows. In Sec. II we present the evolution equations for the two-scalar-field cosmological model. Section III and Appendix A are devoted to the stability analysis of the critical points of the dynamical system arising in our cosmological model. In Sec. IV we interpret the results of this analysis and identify all solutions that correspond to viable cosmological scenarios. Finally, in Sec. V, we present our conclusions.

II. TWO-SCALAR-FIELD COSMOLOGICAL MODEL

Let us consider a cosmological model described by action (1). Varying this action with respect to $g_{\mu\nu}$, ϕ and ξ and assuming a flat Friedmann–Lemaître–Robertson–Walker metric², we obtain the Einstein equations for the scale factor $a(t)$

$$\left(\frac{\dot{a}}{a}\right)^2 = \frac{\kappa^2}{3} \left(\frac{\dot{\phi}^2}{2} + \frac{\dot{\xi}^2}{2} e^{-\alpha\kappa\phi} + V e^{-\beta\kappa\phi} \right), \quad (2)$$

$$\frac{\ddot{a}}{a} = -\frac{\kappa^2}{3} \left(\dot{\phi}^2 + \dot{\xi}^2 e^{-\alpha\kappa\phi} - V e^{-\beta\kappa\phi} \right), \quad (3)$$

and the equations of motion for the scalar fields $\xi(t)$ and $\phi(t)$

$$\ddot{\xi} + 3\frac{\dot{a}}{a}\dot{\xi} - \alpha\kappa\dot{\phi}\dot{\xi} + \frac{\partial V}{\partial \xi} e^{(\alpha-\beta)\kappa\phi} = 0, \quad (4)$$

$$\ddot{\phi} + 3\frac{\dot{a}}{a}\dot{\phi} + \frac{\alpha\kappa}{2}\dot{\xi}^2 e^{-\alpha\kappa\phi} - \beta\kappa V e^{-\beta\kappa\phi} = 0, \quad (5)$$

where an overdot denotes a derivative with respect to time t . These two last equations differ from the usual ones in that they contain an extra term arising due to the presence in action (1) of a nonstandard kinetic term for the scalar field ξ ; the usual equations are recovered for $\alpha = 0$.

Choosing the potential $V(\xi)$ to be of the form

$$V(\xi) = V_a + \frac{1}{2}m^2\xi^2, \quad (6)$$

where V_a and m are constants, and defining the energy density and pressure of the scalar fields as

$$\rho_\xi = \frac{\dot{\xi}^2}{2} e^{-\alpha\kappa\phi} + \frac{1}{2}m^2 e^{-\beta\kappa\phi} \xi^2, \quad (7)$$

$$\rho_\phi = \frac{\dot{\phi}^2}{2} + V_a e^{-\beta\kappa\phi}, \quad (8)$$

and

$$p_\xi = \frac{\dot{\xi}^2}{2} e^{-\alpha\kappa\phi} - \frac{1}{2}m^2 e^{-\beta\kappa\phi} \xi^2, \quad (9)$$

$$p_\phi = \frac{\dot{\phi}^2}{2} - V_a e^{-\beta\kappa\phi}, \quad (10)$$

we can write Eq. (4) for the scalar field ξ as

$$\dot{\rho}_\xi + 3H(\rho_\xi + p_\xi) = \frac{\kappa}{2} \left(\alpha \dot{\xi}^2 e^{-\alpha\kappa\phi} - \beta m^2 \xi^2 e^{-\beta\kappa\phi} \right) \dot{\phi}, \quad (11)$$

where $H = \dot{a}/a$ is the Hubble parameter.

Let us now assume that the scalar field ξ oscillates rapidly around the minimum of its potential, thus behaving like a nonrelativistic dark-matter fluid with an equation of state $\langle p_\xi \rangle = 0$, where the brackets $\langle \dots \rangle$ denote the average over an oscillation period. Then, averaging over an oscillation and taking into account that $\langle p_\xi \rangle = 0$ implies $\langle \xi^2 \rangle = \rho_\xi m^{-2} e^{\beta\kappa\phi}$ and $\langle \dot{\xi}^2 \rangle = \rho_\xi e^{\alpha\kappa\phi}$, the evolution equations become

$$\dot{\rho}_\xi + 3H\rho_\xi = \frac{\kappa}{2}(\alpha - \beta)\rho_\xi\dot{\phi}, \quad (12)$$

$$\ddot{\phi} + 3H\dot{\phi} - \beta\kappa V_a e^{-\beta\kappa\phi} = -\frac{\kappa}{2}(\alpha - \beta)\rho_\xi, \quad (13)$$

$$\dot{H} = -\frac{\kappa}{2}(\dot{\phi}^2 + \rho_\xi), \quad (14)$$

subject to the Friedmann constraint

$$H^2 = \frac{\kappa^2}{3} \left(\frac{\dot{\phi}^2}{2} + V_a e^{-\beta\kappa\phi} + \rho_\xi \right). \quad (15)$$

In previous work [15], we have shown that this two-scalar-field cosmological model allows for a unified description of inflation, dark matter, and dark energy, in which the scalar field ξ plays the roles of both inflaton and dark matter, while the scalar field ϕ plays the role of dark energy³. There, the solution of Eq. (12),

$$\rho_\xi = \rho_{\xi,0} \left(\frac{a_0}{a} \right)^3 e^{\frac{\kappa}{2}(\alpha-\beta)(\phi-\phi_0)}, \quad (16)$$

where the subscript 0 denotes present-time quantities, was inserted into Eqs. (13)–(15) and the resulting system was solved numerically for specific values of α and β .

² Because the curvature density parameter Ω_k is constrained by current cosmological measurements to be very small [3], we can assume a spatially flat metric without much loss of generality.

³ In the specific case $\alpha = \sqrt{6}/3$ and arbitrary β , corresponding to a generalized hybrid metric-Palatini theory of gravity, a unified description of dark matter and dark energy—but not inflation—was proposed in Ref. [22].

In the present article, instead of numerical methods, we use methods of qualitative analysis of dynamical systems to investigate the solutions of Eqs. (12)–(15), covering now the entire parameter space (α, β) .

To conclude this section, let us point out that the two-scalar-field cosmological model under consideration admits a direct transfer of energy between dark energy and dark matter, mediated by the term

$$Q = \frac{\kappa}{2}(\alpha - \beta)\rho_\xi \dot{\phi}, \quad (17)$$

as results from Eqs. (12) and (13).

Cosmological models with an interaction term $Q \propto \rho \dot{\phi}$, where ϕ is a scalar field with an exponential potential and ρ is the energy density of a perfect fluid with an equation of state $p = w\rho$, have been investigated by several authors [23–32]; for other interaction terms considered in dark-matter and dark-energy interaction models, see the review articles [33, 34].

What is rather interesting in the interaction term Q given by Eq. (17) is that it vanishes for $\alpha = \beta$. This means that the transfer of energy between two scalar fields directly coupled via an exponential potential can be canceled due to the presence of a nonstandard kinetic term. In this case, the energy density of dark matter ρ_ξ evolves as a^{-3} [see Eq. (16)], i.e., exactly as ordinary baryonic matter, while dark energy evolves subject only to the potential $V_a e^{-\kappa\beta\phi}$. In what follows, we will consider this case, but also the case $\alpha \neq \beta$ for which there is a direct energy exchange between the two scalar fields.

III. DYNAMICAL-SYSTEM ANALYSIS

Let us now turn to the analysis of the system of differential equations (12)–(15) using methods of qualitative analysis of dynamical systems (for a recent review on dynamical systems applied to cosmology and, in particular, to dark-energy models, see Ref. [35]).

Following Ref. [36], we introduce the dimensionless variables,

$$x^2 = \frac{\kappa^2}{6H^2} \dot{\phi}^2 \quad \text{and} \quad y^2 = \frac{\kappa^2}{3H^2} V_a e^{-\beta\kappa\phi}, \quad (18)$$

as well as a new time variable τ , defined as

$$\tau = \ln a, \quad \frac{d\tau}{dt} = H. \quad (19)$$

In these new variables, the system of equations (12)–(15) can be written as

$$x' = -3x + \frac{\sqrt{6}}{2}\beta y^2 + \frac{3}{2}x(1+x^2-y^2) - \frac{\sqrt{6}}{4}(\alpha-\beta)(1-x^2-y^2), \quad (20a)$$

$$y' = -\frac{\sqrt{6}}{2}\beta xy + \frac{3}{2}y(1+x^2-y^2), \quad (20b)$$

where the prime denotes a derivative with respect to the logarithmic time τ . Notice that the Friedmann constraint, given by

$$x^2 + y^2 + \Omega_\xi = 1, \quad \Omega_\xi \equiv \rho_\xi \frac{\kappa^2}{3H^2}, \quad (21)$$

was used in Eqs. (20) to eliminate the explicit dependence on the variable ρ_ξ , thus reducing the dynamical system to just two dimensions, a circumstance that considerably simplifies the analysis.

Because the density parameter Ω_ξ is, by definition, non-negative and we are assuming a flat universe, it follows from the Friedmann constraint (21) that the variables x and y should satisfy the condition $x^2 + y^2 \leq 1$, i.e., the physically relevant orbits of the dynamical system (20) are confined to the unit circle. Furthermore, since we are interested in expanding cosmologies, the analysis should be restricted to the upper semicircle, for which $y \geq 0$. In summary, the phase space of the dynamical system (20) is the upper half of the unit circle centered at the origin.

The dynamical system (20) contains two dimensionless constants α and β , which parameterize the nonstandard kinetic term of the scalar field ξ and the interaction potential between the scalar fields ϕ and ξ , respectively [see action (1)]. Without any loss of generality, we can assume that α is non-negative⁴. Furthermore, the case $\alpha = 0$, corresponding to an action with a standard kinetic term for the scalar field ξ , has been extensively studied in the literature [35] and, therefore, will not be considered in this article. In what concerns β , we allow it to take any value, including the value zero, for which the direct coupling in the potential between the two scalar fields vanishes. In summary, the parameters α and β span the open half-plane $\alpha > 0$.

Depending on the values of α and β , the dynamical system (20) has up to five critical points. Table I and Fig. 1 summarize, in both analytical and graphical form, the conditions for their existence and stability, as well as the conditions for the existence of accelerated solutions.

For most values of α and β , the stability of the critical points can be assessed simply by using the linear theory, since, for those values, both eigenvalues of the Jacobian matrix of the dynamical system (20) have a nonzero real part. However, for certain values of α and β , namely, $\beta = \alpha \pm \sqrt{6}$, $\beta = \sqrt{\alpha^2 + 6}$, $\beta = \pm\sqrt{6}$, and $\beta = (-\alpha + \sqrt{\alpha^2 + 24})/2$, corresponding to the lines delimiting the different regions of the plots of Fig. 1, one of the eigenvalues becomes zero, forcing us to go beyond the linear theory and use other methods to study the

⁴ Indeed, since the dynamical system (20) is invariant under the transformation $x \rightarrow -x$, $\alpha \rightarrow -\alpha$, and $\beta \rightarrow -\beta$, solutions for negative values of α (β) can be obtained straightforwardly from solutions for positive values of α (β), provided a reflection over x is performed, as well as a change of sign of the parameter β (α).

Point	x	y	Existence	Stability	Acceleration
A	1	0	$\forall \alpha, \beta$	$\beta \geq \alpha + \sqrt{6}$	never
B	-1	0	$\forall \alpha, \beta$	$\beta \leq -\sqrt{6}$	never
C	$\frac{\beta - \alpha}{\sqrt{6}}$	0	$ \alpha - \beta \leq \sqrt{6}$	$\sqrt{\alpha^2 + 6} \leq \beta \leq \alpha + \sqrt{6}$	never
D	$\frac{\beta}{\sqrt{6}}$	$\sqrt{1 - \frac{\beta^2}{6}}$	$ \beta \leq \sqrt{6}$	$-\sqrt{6} \leq \beta \leq \frac{-\alpha + \sqrt{\alpha^2 + 24}}{2}$	$ \beta < \sqrt{2}$
E	$\frac{\sqrt{6}}{\alpha + \beta}$	$\frac{\sqrt{6 + \alpha^2 - \beta^2}}{\alpha + \beta}$	$-\alpha + \frac{\sqrt{\alpha^2 + 24}}{2} \leq \beta \leq \sqrt{\alpha^2 + 6}$	$-\alpha + \frac{\sqrt{\alpha^2 + 24}}{2} \leq \beta \leq \sqrt{\alpha^2 + 6}$	$\beta < \frac{\alpha}{2}$

TABLE I: Properties of the critical points of the dynamical system (20): existence, stability, and acceleration.

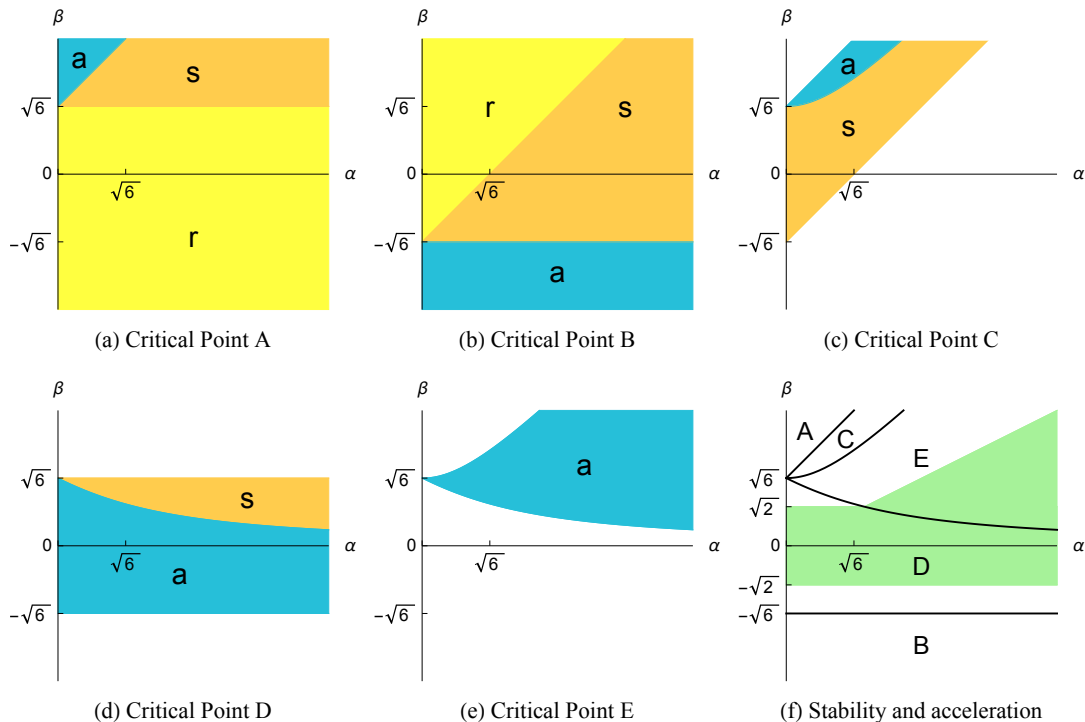


FIG. 1: Panels (a) to (e) show the regions of existence and stability of the critical points of the dynamical system (20) in the parameter space (α, β) —the open half-plane $\alpha > 0$. In white regions, critical points do not exist. In blue (dark shaded) regions they exist and are stable (attractors), while in orange (medium shaded) and yellow (lightly shaded) regions they exist, but are unstable (saddles and repellers, respectively). The regions in which the critical points are attractors, saddles, and repellers, are also denoted by the letters “a”, “s”, and “r”, respectively. Panel (f) shows the parameter space divided into five regions, in each of which one and only one of the critical points A, B, C, D, and E is an attractor. The part of the parameter space in which critical point D (or critical point E) is an attractor and, simultaneously, corresponds to a state of accelerated expansion is highlighted in green color (shaded).

stability properties of the critical points, such as center manifold theory and Lyapunov’s method. In Appendix A we present a full analysis of the stability of the five critical points for all values of α and β belonging to the parameter space.

Note that each of the critical points is stable for specific values of α and β and that to each point of the parameter space (α, β) corresponds one and only one stable critical point (see Fig. 1).

The existence and stability conditions for the critical points allow for a division of the parameter space (α, β) into nine regions (see Fig. 2 and Table II), each of which

corresponds to a qualitatively different phase portrait. Nine phase portraits, representative of the behavior of the dynamical system (20) in each of these regions, are shown in Fig. 3.

Since there is only one attracting critical point in each region, all orbits of the corresponding phase portraits (except the heteroclinic ones connecting the other critical points) asymptotically converge to this unique attractor, which, therefore, represents the final stage of evolution of the Universe. The phase portraits corresponding to regions II to VIII always contain at least one saddle point (see Table II). The repellers are always critical points A

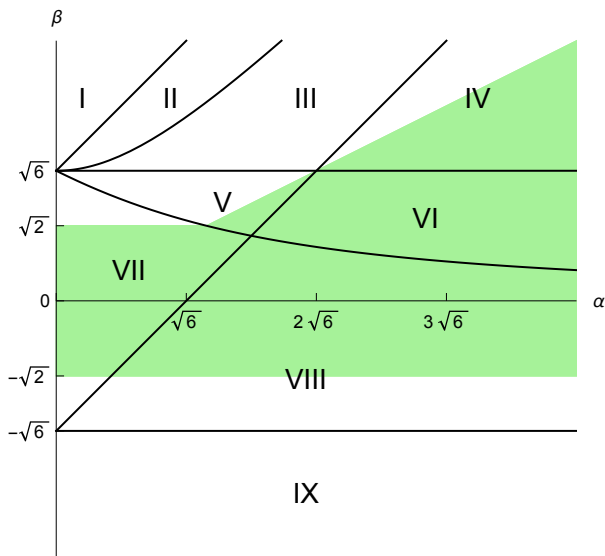


FIG. 2: The existence and stability conditions of the critical points allow for a division of the parameter space (α, β) into nine regions, labeled with Roman numerals, each of which corresponds to a qualitatively different phase portrait of the dynamical system (20). In green color (shaded) it is indicated the regions or part of them in which critical point D (or critical point E) is an attractor and, simultaneously, corresponds to a state of accelerated expansion.

Point	I	II	III	IV	V	VI	VII	VIII	IX
A	a	s	s	s	r	r	r	r	r
B	r	r	r	s	r	s	r	s	a
C		a	s		s		s		
D					s	s	a	a	
E			a	a	a	a			

TABLE II: Division of the parameter space (α, β) into nine regions, labeled with Roman numerals. For each such region, the critical points are classified using the letters “a”, “s”, and “r”, denoting attractor, saddle, and repeller, respectively. The absence of a letter means that the corresponding critical point does not exist in that region.

and/or B. The exception is the phase portrait of region IV, which has no repellers at all; for $\tau \rightarrow -\infty$, all orbits approach the heteroclinic one connecting critical points A and B through the x -axis and the upper half of the circumference $x^2 + y^2 = 1$. In regions V and VII, the phase portraits have two repellers, critical points A and B. In this case, the phase space is divided into two parts by the heteroclinic orbit connecting points C, D, and E (region V) and points C and D (region VII); orbits on the right part of the phase space originate at critical point A, while on the left they have their origin at critical point B.

Before proceeding to the physical interpretation of the results obtained in this section, let us point out that,

Point	Ω_ϕ	Ω_ξ	w_{eff}
A	1	0	1
B	1	0	1
C	$\frac{(\alpha-\beta)^2}{6}$	$1 - \frac{(\alpha-\beta)^2}{6}$	$\frac{(\alpha-\beta)^2}{6}$
D	1	0	$-1 + \frac{\beta^2}{3}$
E	$\frac{12+\alpha^2-\beta^2}{(\alpha+\beta)^2}$	$\frac{2(\alpha\beta+\beta^2-6)}{(\alpha+\beta)^2}$	$\frac{-\alpha+\beta}{\alpha+\beta}$

TABLE III: Density parameters for dark energy and dark matter and the effective equation-of-state parameter for the critical points of the dynamical system (20).

in the variables x and y , the density parameter for the scalar field ϕ , the effective equation-of-state parameter, and the deceleration parameter, are given by

$$\Omega_\phi \equiv \rho_\phi \frac{\kappa^2}{3H^2} = x^2 + y^2, \quad (22)$$

$$w_{\text{eff}} \equiv \frac{p_\xi + p_\phi}{\rho_\xi + \rho_\phi} = x^2 - y^2, \quad (23)$$

and

$$q \equiv -\frac{H'}{H} - 1 = \frac{1}{2} (1 + 3x^2 - 3y^2), \quad (24)$$

respectively.

For certain values of α and β , critical points D and E correspond to a state in which the deceleration parameter q is negative. In the phase space (x, y) , this region of negative q lies above the curve $y = \sqrt{x^2 + 1/3}$ (see Fig. 3); orbits inside this region correspond to a state of accelerated expansion of the Universe. The regions of the parameter space (α, β) in which critical points D and E are attractors and, simultaneously, correspond to a state of accelerated expansion are shown in panel (f) of Fig. 1 and in Fig. 2.

IV. COSMOLOGICAL SOLUTIONS

Let us now proceed to the physical interpretation of the results obtained in Sec. III.

Critical points A and B correspond to a state of the Universe in which the total energy density $\rho = \rho_\xi + \rho_\phi$ is dominated by the kinetic term of the scalar field ϕ ($\Omega_\phi = 1$), which, therefore, behaves as a stiff-matter fluid ($w_{\text{eff}} = 1$). The density parameter Ω_ξ vanishes, meaning that the influence of the scalar field ξ on the dynamics of the Universe is negligible in the vicinity of these critical points (see Table III).

At critical point C, the state of the Universe depends crucially on the values of the parameters α and β . For $\alpha = \beta$, the dark-matter field ξ dominates the evolution of the Universe ($\Omega_\xi = 1$). For $\beta = \alpha \pm \sqrt{6}$, corresponding

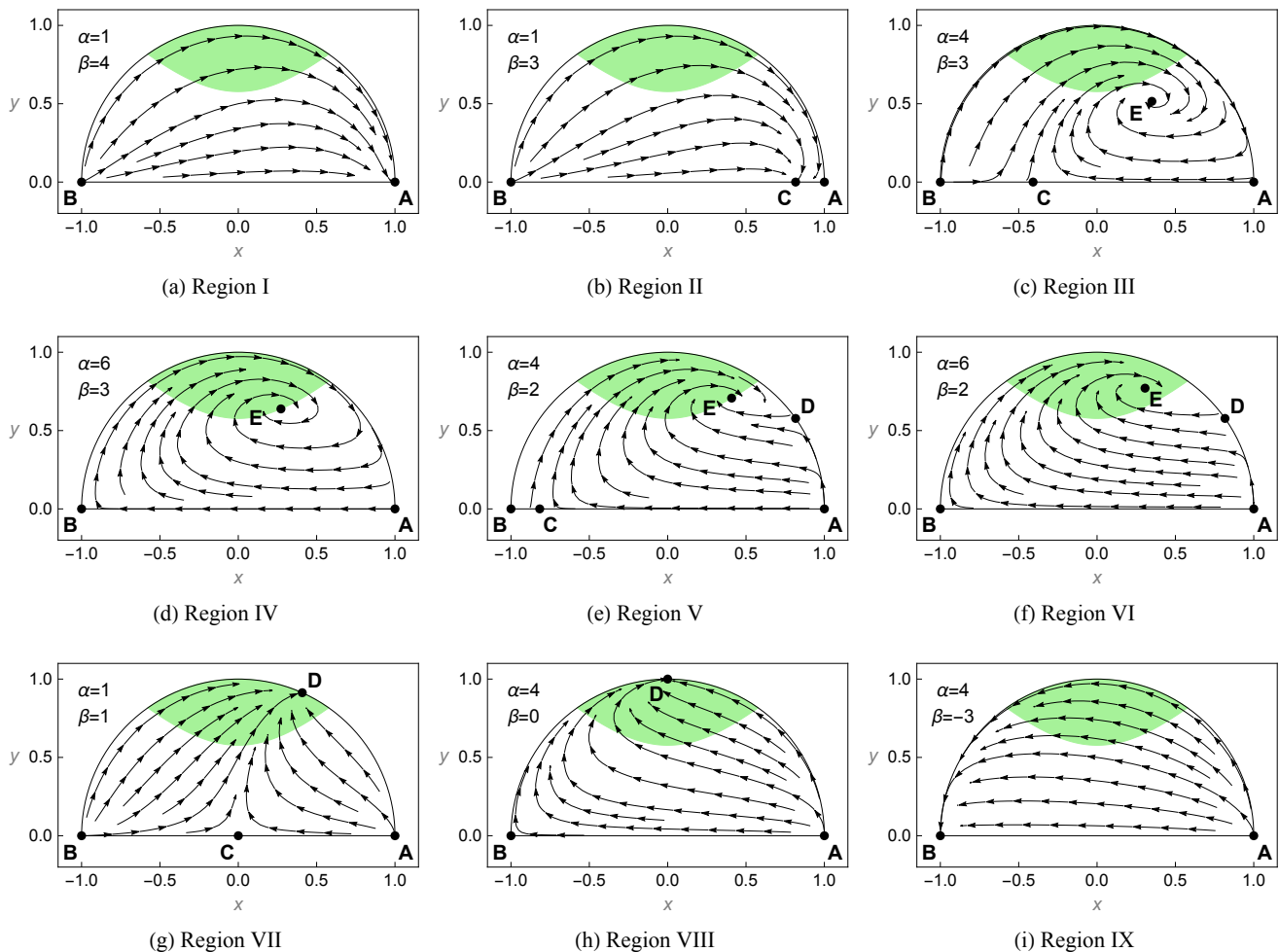


FIG. 3: Phase portraits of the dynamical system (20) for different values of the parameters α and β . Each of these phase portraits corresponds to one of the nine regions of the parameter space shown in Fig. 2 (see also Table II). In the green (shaded) region of phase space the expansion of the Universe is accelerated.

to the lines delimiting the region of existence of this critical point, it is the kinetic term of the scalar field ϕ that dominates ($\Omega_\phi = 1$), leading to a stiff-matter behavior. For intermediate values of the difference $\alpha - \beta$, neither ξ nor ϕ entirely dominate the evolution of the Universe, and, consequently, the effective equation-of-state parameter w_{eff} can take any value in the range 0 to 1, depending on the relative preponderance of the scalar fields. Of particular relevance is the case in which critical point C is a saddle and ξ is the dominant field (such behavior may occur in regions III, V, and VII of the parameter space); it corresponds to a transitory period of matter domination in the history of the Universe, needed for structure formation. Although of lesser relevance, let us note that critical point C can also be an attractor (in region II of the parameter space), in which case the ratio Ω_ϕ/Ω_ξ between the density parameters of the scalar fields becomes locked, asymptotically, at a constant value determined by α and β (see Table III).

At critical point D, which exists for $|\beta| \leq \sqrt{6}$, the

evolution of the Universe is dominated by the scalar field ϕ ($\Omega_\phi = 1$). The effective equation-of-state parameter w_{eff} depends just on β and can take any value from -1 to 1 , reflecting the relative preponderance of the potential and kinetic energies of the field ϕ on the total energy density of the Universe. More specifically, for $\beta = 0$ the potential term $V_a e^{-\beta\kappa\phi}$ is preponderant and the scalar field ϕ behaves like a cosmological constant ($w_{\text{eff}} = -1$), giving rise to a period of accelerated expansion of the Universe; for $\beta = \pm\sqrt{6}$, it is the kinetic term $\dot{\phi}^2/2$ that dominates and the scalar field behaves as a stiff-matter fluid ($w_{\text{eff}} = 1$). Here, the most interesting situation is the one in which critical point D corresponds to a state of accelerated expansion ($w_{\text{eff}} < -1/3$), occurring for $|\beta| < \sqrt{2}$.

At critical point E, which is always an attractor, the evolution of the Universe can be dominated by either ϕ or ξ , depending on the values of α and β . For $\beta = (\sqrt{\alpha^2 + 24} - \alpha)/2$ [lower boundary of the region of existence of critical point E, see panel (e) of Fig. 1],

the evolution of the Universe is dominated by the potential term of the scalar field ϕ as α tends to infinity ($\Omega_\phi = 1$, $w_{\text{eff}} = -1$). For $\beta = \sqrt{\alpha^2 + 6}$ (upper boundary), it is the scalar field ξ that dominates the evolution for $\alpha \rightarrow +\infty$ ($\Omega_\xi = 1$, $w_{\text{eff}} = 0$). As one approaches the point of intersection of these two curves, at $(0, \sqrt{6})$, the evolution becomes dominated by the kinetic term of ϕ ($\Omega_\phi = 1$, $w_{\text{eff}} = 1$). Here, again, the most interesting case is the one for which critical point E corresponds to a state of accelerated expansion ($w_{\text{eff}} < -1/3$), occurring for values of α and β lying in the region of the parameter space delimited by the curves $2\beta < \alpha$ and $\beta = (\sqrt{\alpha^2 + 24} - \alpha)/2$ [see panel (f) of Fig. 1]. Once this critical point is reached, the ratio between the density parameters of the scalar fields is locked at a constant value which depends on α and β , namely,

$$\frac{\Omega_\phi}{\Omega_\xi} = \frac{12 + \alpha^2 - \beta^2}{2(\alpha\beta + \beta^2 - 6)}. \quad (25)$$

This is the so-called scaling solution, first discussed in Ref. [37] and often used to try to solve the coincidence problem.

Having identified the physical nature of the critical points of the dynamical system (20), let us now proceed to the description of the phase portraits shown in Fig. 3, which are representative of each of the nine regions of the parameter space.

In region I of the parameter space (α, β) , the dynamical system (20) has only two critical points, A and B, which are an attractor and a repeller, respectively. All orbits start on B and end on A, some of them passing through the zone of the phase space in which the Universe expansion is accelerated [see panel (a) of Fig. 3]. Therefore, the initial and final states of the Universe are of stiff-matter domination with a possible intermediate stage of accelerated expansion.

In region II, all orbits originate at critical point B and end at critical point C (except for the orbits connecting the B to A and A to C through the boundaries of the phase space), some of them passing in the acceleration zone and near the saddle point A [see panel (b) of Fig. 3]. Therefore, the Universe goes from a stiff-matter initial state—sometimes through an intermediate stage of accelerated expansion—to a final state dominated by a scalar field which, depending on the values of α and β , has a behavior ranging from dust to stiff matter.

In region III, the attractor is now critical point E, while point B is a repeller and both A and C are saddle points. Some of the orbits approach C (which may correspond to a matter-dominated state for certain values of α and β), before heading to the attractor E [see panel (c) of Fig. 3]. Although critical point E is always located outside the acceleration zone, some orbits approaching this point may pass through this zone, giving rise to a temporary period of accelerated expansion.

In region IV, the phase space has no repelling critical points; for $\tau \rightarrow -\infty$, all orbits approach the heteroclinic one connecting critical points A and B through

the boundaries of the phase space. An orbit originating, for instance, near critical point A, heads to the vicinity of point B, before spiraling to the attractor E [see panel (d) of Fig. 3], which may correspond to an accelerated solution if $2\beta < \alpha$.

Region V is the only region of the parameter space for which the corresponding phase portrait has five critical points (see Table II). Critical point E is again the attractor, which corresponds to a scaling solution. Critical points A and B are repellers, near which the dominant scalar field ϕ behaves as stiff matter. Critical points C and D are both saddle points. In the vicinity of C, the scalar field ξ may be preponderant, giving rise to a matter-dominated era. In what concerns critical point D, it may correspond to a state of (temporary) accelerated expansion, with $-1/2 < w_{\text{eff}} < -1/3$, if $\beta < \sqrt{2}$. Some orbits, originating at points A or B, first approach C and then head to E through the accelerating zone [see panel (e) of Fig. 3]. If critical point E lies inside this zone, accelerated expansion is the final state of the Universe; otherwise, accelerated expansion is just a temporary stage, before the Universe evolves to a final state in which $-1/3 < w_{\text{eff}} < 1$.

In region VI, critical point E is again the attractor, which always corresponds to an accelerated scaling solution. The repelling critical point is A, while B and D are saddles. Orbits originating near point A, first approach B, before heading to E [see panel (f) of Fig. 3]. Note that critical point C does not exist in this region of the parameter space; therefore, the Universe cannot experience an intermediate era of matter domination.

In region VII, the attractor is critical point D, which corresponds to a state of everlasting accelerated expansion for $|\beta| < \sqrt{2}$. Point C is a saddle, near which the dynamics may be dominated by the scalar field ξ . All orbits originating in repelling points A and B (except for the heteroclinic orbits connecting points A and B to C) end up at critical point D [see panel (g) of Fig. 3]. Of particular interest are those orbits that, before heading to D, closely approach point C. In this case, the final state of accelerated expansion may be preceded by a long period of dark-matter domination.

In region VIII, the final stage of evolution of the Universe corresponds to critical point D, which, for $\beta > -\sqrt{2}$, is again an accelerated solution. The repeller is critical point A, from which all orbits originate (except for the heteroclinic orbit connecting points B and D through the boundary of the phase space). Some of the orbits leaving critical point A first approach B, before heading to D [see panel (h) of Fig. 3].

Finally, in region IX, the situation is similar to that of region I, but with critical points A and B reversing their roles [see panel (i) of Fig. 3].

At this point a comment is in order. For clarity of presentation and easier interpretation of the roles played by each of the two scalar fields in the cosmic evolution, we have chosen not to overload the equations of motion with radiation and ordinary baryonic matter. In particular,

the inclusion of these two components would increase the number of equations of the dynamical system describing our cosmological model, and, consequently, would make its analysis and interpretation technically more demanding and conceptually less clear. But since the Universe has had a radiation-dominated era in the past and contains, in addition to dark matter, ordinary baryonic matter, we should, when further analyzing the phase portraits corresponding to the different regions of the parameter space, focus our attention on the later phases of the cosmic evolution and ignore the early phases, which, as we have seen, correspond to a stiff-matter state (reflecting the fact that the repellers are always the critical points A and B, for which $w_{\text{eff}} = 1$). Therefore, in what follows, we assume that the Universe has undergone an inflationary period, followed by a long enough radiation-dominated era encompassing the nucleosynthesis period, and that the subsequent evolution is described by the later stages of our two-scalar-field cosmological model, in which the scalar field ξ accounts for all (dark and baryonic) matter content (yielding $\Omega_{\xi,0} \approx 0.31$) and the scalar field ϕ accounts for dark energy (with $\Omega_{\phi,0} \approx 0.69$).

For our model to reproduce the main features of the evolution of the observed Universe, we should search for solutions of the dynamical system (20) having an intermediate matter-dominated era, long enough to allow for structure formation, followed by a present era of (everlasting or temporary) accelerated expansion.

Let us start by noting that, at critical point C, the density parameter of the scalar field ξ is given by

$$\Omega_{\xi} = 1 - \frac{(\alpha - \beta)^2}{6}, \quad (26)$$

implying that this critical point corresponds to a state of matter domination only if the difference between the parameters α and β is small enough. In Ref. [15] it has been shown, resorting to numerical simulations, that α and β should satisfy the condition $|\alpha - \beta| \lesssim 1$ to ensure that the transition between the radiation- and matter-dominated eras does not occur too early in the cosmic history, thus avoiding a conflict with primordial nucleosynthesis. In what follows, we adopt this upper limit, which implies $\Omega_{\xi} \gtrsim 5/6$ and $w_{\text{eff}} \lesssim 1/6$ at critical point C. This choice restricts the relevant solutions to regions III, V, and VII of the parameter space, the only ones that overlap, even if only partially, with the strip defined by $|\alpha - \beta| \lesssim 1$.

In these three regions of the parameter space, for an appropriate choice of α and β , the matter-dominated era may be followed by a period of accelerated expansion.

In region III, the attractor E is always located outside the acceleration zone, implying that accelerated expansion can only be temporary (corresponding to phase-space orbits that, before heading to point E, pass through the acceleration zone). These temporary accelerated solutions only exist for points of the parameter space (α, β) sufficiently close to the line $2\beta = \alpha$. This condition, together with the condition $|\alpha - \beta| \lesssim 1$, severely restricts the values of α and β for which the Universe experiences

a (temporary) period of accelerated expansion.

In region V, the attractor E could be chosen to lie inside the acceleration zone, but the corresponding values of α and β would then not satisfy the condition $|\alpha - \beta| \lesssim 1$; therefore, this attractor should lie outside the acceleration zone and, again, the state of accelerated expansion can only be temporary. However, in this case, the restriction to the allowed values of α and β is not as strong as in region III.

Finally, in region VII, the attractor D corresponds to a state of everlasting accelerated expansion for $|\beta| < \sqrt{2}$. This condition, conjugated with $|\alpha - \beta| \lesssim 1$, allows for a wide choice of values of α and β giving rise to cosmological solutions with the required features. In this region of the parameter space, temporary accelerated solutions can also be found for values of β slightly above $\sqrt{2}$ (attractor D slightly outside the acceleration zone).

In summary, among the multitude of cosmological solutions of our two-scalar-field model, those reproducing the main features of the Universe's evolution lie in regions III, V, and VII of the parameter space. There, for an appropriate choice of α and β , the scalar field ξ , which behaves as cold dark matter, dominates the evolution of the Universe for enough time to allow for structure formation; this stage of evolution is then followed by an era of accelerated expansion—temporary or permanent—driven by the scalar field ϕ , which, therefore, behaves like dark energy.

The evolution of the density parameters Ω_{ϕ} and Ω_{ξ} , as well as the evolution of the effective equation-of-state parameter w_{eff} , for different values of α and β belonging to regions III, V, and VII of the space parameter, is shown in Fig. 4. In all cases, we choose initial conditions guaranteeing that the transition from matter to dark-energy domination occurs in a recent past, namely, for $\tau \approx -0.5$, and also that, at the present time $\tau = 0$, the value of the density parameter of the scalar field ϕ is in agreement with cosmological measurements [3], namely, $\Omega_{\phi,0} \approx 0.69$. In regions III and V, because the attractor is critical point E, the ratio $\Omega_{\phi}/\Omega_{\xi}$ tends, in the future, to a constant value, that depends on α and β . On the contrary, in region VII, where the attractor is critical point D, the energy density of the dark-matter field rapidly approaches zero, independently of the values of α and β ; consequently, in the future, the Universe becomes entirely dominated by the dark-energy field. In all the cases considered in Fig. 4, the effective equation-of-state parameter at present is smaller than $-1/3$, signaling an accelerated growth of the scale factor of the Universe. In regions III and V, this accelerated expansion is only temporary; in the future, w_{eff} approaches the quantity $(\beta - \alpha)/(\alpha + \beta)$, which, for the chosen values of α and β , is always greater than $-1/3$. On the contrary, in region VII, the asymptotic value of the effective equation-of-state parameter depends only on β , namely, $w = -1 + \beta^2/3$, implying that, for $|\beta| < \sqrt{2}$, the accelerated expansion of the Universe lasts forever.

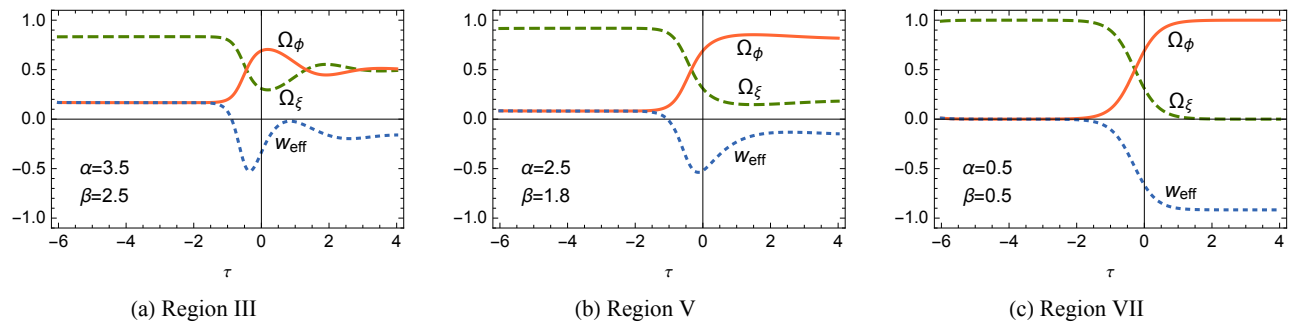


FIG. 4: Evolution of Ω_ϕ , Ω_ξ , and w_{eff} for values of α and β belonging to regions III, V, and VII of the parameter space. At the present time, $\tau = 0$, the density parameters are $\Omega_{\phi,0} \approx 0.69$ and $\Omega_{\xi,0} \approx 0.31$ in all cases, while the effective equation-of-state parameter is $w_{\text{eff},0} \approx -0.34$, -0.52 , and -0.66 for the cases shown in panels (a), (b), and (c), respectively. In regions III and V, the attractor is critical point E, implying that, for $\tau \rightarrow +\infty$, the ratio between the density parameters approaches a constant value [$\Omega_\phi/\Omega_\xi = 1$ and 4.3 for the cases shown in panels (a) and (b), respectively]. In region VII, where the attractor is critical point D, the energy density of the dark-matter field ξ quickly approaches zero for $\tau > 0$ and, consequently, the evolution of the Universe becomes entirely dominated by the dark-energy field ϕ .

V. CONCLUSIONS

In this article, we have investigated the late-time evolution of the Universe within a cosmological model in which dark matter and dark energy are identified with two interacting scalar fields. More specifically, we assume that one of the scalar fields, ξ , oscillates rapidly around the minimum of its quadratic potential, thus behaving like a dark-matter fluid, while the other scalar field, ϕ , evolving under an exponential potential, gives rise to the current era of accelerated cosmic expansion, thus behaving like dark energy.

As shown in Ref. [15], this two-scalar-field cosmological model admits viable scenarios for the evolution of the Universe. More specifically, upon certain assumptions and an appropriate choice of the parameters α and β , it is possible to obtain a correct sequence of eras in the evolution of the Universe, namely, an inflationary era driven by the scalar field ξ , a radiation-dominated era encompassing the primordial nucleosynthesis period, an era dominated by the dark-matter field ξ and, to a lesser extent, by ordinary baryonic matter, long enough to allow for structure formation, and, finally, a current era of accelerated expansion driven by the dark-energy field ϕ .

Our previous investigations of this two-scalar-field cosmological model [15, 22] resorted to numerical methods to solve the evolution equations and, consequently, have not covered the entire parameter space. To fill this gap, we have now turned to the powerful methods of qualitative analysis of dynamical systems, applied with great success to astrophysical and cosmological problems for several decades. With such methods, it is possible to cover the entire parameter space (α, β) and, therefore, ensure that all cosmological solutions of interest are identified.

Because of the symmetries of action (1), the parameter space can be restricted, without any loss of generality, to

either the half-plane $\beta \geq 0$ or the half-plane $\alpha \geq 0$. We have chosen the latter possibility and, in addition, opted not to consider the case $\alpha = 0$, corresponding to an action with a standard kinetic term for the scalar field ξ , since this case has been extensively studied in the literature. Therefore, in our dynamical-system analysis, the parameters α and β span the open half-plane $\alpha > 0$.

In this work, we have chosen not to overload the evolution equations (12)–(15) with radiation and ordinary baryonic matter, in order to better highlight the roles played by the scalar fields ξ and ϕ as dark matter and dark energy. Having made this choice, we focused our attention on the later phases of cosmic evolution—the eras dominated by dark matter and dark energy—, assuming that previously the Universe has undergone an inflationary period and a radiation-dominated era.

The two-dimensional dynamical system (20), arising from the evolution equations (12)–(15), admits five critical points, whose stability properties were investigated within the linear theory and, when this was not feasible, resorting to the center manifold theory and Lyapunov’s method. This stability analysis, carried out for all possible values of α and β , has shown that the parameter space is naturally divided into nine regions (see Fig. 2 and Table II), each of which corresponds to a qualitatively different phase portrait of the dynamical system.

We have shown that viable solutions—in the sense that they correspond to a cosmic evolution in which a long enough matter-dominated era is followed by a current era of accelerated expansion—can be found in regions III, V, and VII of the parameter space.

Two distinct possibilities have been identified. First, in region VII, the Universe, after a matter-dominated era, evolves to a state of everlasting accelerated expansion, in which the energy density of the dark-matter field rapidly approaches zero and, consequently, the evolution becomes entirely dominated by the dark-energy field [see panel (c) of Fig. 4]. Second, in regions III and V,

the stage of accelerated expansion following the matter-dominated era is always temporary and, for $\tau \rightarrow +\infty$, the ratio between the energy densities of dark energy and dark matter, given by Eq. (25), tends to a nonzero value [see panels (a) and (b) of Fig. 4].

In both cases, the values of α and β should satisfy the condition $|\alpha - \beta| \lesssim 1$ to ensure that the transition between the radiation- and matter-dominated eras does not occur too early in the cosmic history, thus avoiding a conflict with primordial nucleosynthesis [15]. In region VII, this condition, conjugated with the condition $|\beta| < \sqrt{2}$ for the existence of a final state of accelerated expansion, allows for a wide choice of values of the parameters α and β giving rise to solutions with the required features. In regions III and V, on the contrary, this condition is more restrictive, limiting to a small set the allowed values of α and β .

The two-scalar-field cosmological model given by action (1), arising in a great variety of theories of gravity, like the Jordan-Brans-Dicke theory, Kaluza-Klein theories, $f(R)$ -gravity, string theories, and hybrid metric-Palatini theories, seems to be quite promising. It allows for a unified description of inflation, dark energy, and dark matter, which is able to reproduce, at least qualitatively, the main features of the evolution of the observed Universe. The results obtained so far within this cosmological model constitute a first step that needs to be taken further; we expect to do so in future publications.

Appendix A: Stability of the critical points

For most values of α and β , linear theory suffices to assess the stability of the critical points of the dynamical system (20). However, for certain values of these parameters, this is not enough and one has to resort to other methods, such as the center manifold theory and Lyapunov's method. For more details on the methods used in this Appendix, the reader is referred to the specialized literature [38–40] and to a recent review on dynamical systems applied to cosmology [35].

1. Critical point A

At critical point A, with coordinates $x = 1$ and $y = 0$, the eigenvalues of the Jacobian matrix of the dynamical system (20) are

$$\lambda_1 = 3 + \frac{\sqrt{6}}{2}(\alpha - \beta) \quad \text{and} \quad \lambda_2 = 3 - \frac{\sqrt{6}}{2}\beta, \quad (\text{A1})$$

implying that for $\beta > \alpha + \sqrt{6}$, $\sqrt{6} < \beta < \alpha + \sqrt{6}$, and $\beta < \sqrt{6}$ the critical point is an attractor, a saddle, and a repeller, respectively [see panel (a) of Fig. 1 and Table II].

For $\beta = \alpha + \sqrt{6}$ and $\beta = \sqrt{6}$ one of the eigenvalues vanishes, forcing us to go beyond the linear theory.

Let us start with the case $\beta = \alpha + \sqrt{6}$, using Lyapunov's method to study the stability of the critical point. Consider the function $V(x, y) = (x - 1)^2 + y^2$, defined in the phase space of the dynamical system (20), i.e., in the upper half of the unit circle centered at the origin ($x^2 + y^2 \leq 1, y \geq 0$). This function is equal to zero at critical point A and positive elsewhere. Furthermore, its derivative,

$$V' = -3(1+x)(1-x)^3 - \sqrt{6}\alpha y^2 - 3y^4, \quad (\text{A2})$$

is negative in the neighborhood of A (recall that the parameter space is the open half-plane $\alpha > 0$). Therefore, we arrive at the conclusion that the critical point is asymptotically stable and the phase-space orbits near it are similar to the ones shown in panel (a) of Fig. 3.

Let us now turn to the case $\beta = \sqrt{6}$. Since the eigenvalue $\lambda_1 = \sqrt{6}\alpha/2$ is positive, the critical point cannot be an attractor. It is either a saddle or a repeller, depending on the behavior of the dynamical system on the center manifold, which we now proceed to investigate. In new variables $u = x - 1$ and $v = y$, which shift the critical point to the origin, the dynamical system (20) becomes

$$u' = \lambda_1 u + f(u, v), \quad (\text{A3a})$$

$$v' = g(u, v), \quad (\text{A3b})$$

where the nonlinear functions f and g are given by

$$f(u, v) = \left(3 + \frac{\sqrt{6}}{4}\alpha\right)u^2 + \frac{\sqrt{6}}{4}\alpha v^2 + \frac{3}{2}u^3 - \frac{3}{2}uv^2, \quad (\text{A4})$$

$$g(u, v) = \frac{3}{2}u^2v - \frac{3}{2}v^3. \quad (\text{A5})$$

The center manifold, obtained as a Taylor series expansion from the equation

$$\frac{dh(v)}{dv}g[h(v), v] - \lambda_1 h(v) - f[h(v), v] = 0, \quad (\text{A6})$$

is given by

$$u = h(v) = -\frac{1}{2}v^2 - \frac{1}{8}v^4 + \mathcal{O}(v^6) \quad (\text{A7})$$

and the flow on it is governed by the differential equation

$$v' = \frac{3}{2}v [h^2(v) - v^2] = -\frac{3}{2}v^3 + \mathcal{O}(v^5). \quad (\text{A8})$$

Therefore, along the v direction the orbits approach the origin, implying that critical point A is a saddle for $\beta = \sqrt{6}$ (recall that along the u direction the orbits move away from critical point A). In the neighborhood of this point, the orbits are similar to the ones shown in panels (b), (c), and (d) of Fig. 3.

In summary, critical point A is an attractor for $\beta \geq \alpha + \sqrt{6}$, a saddle for $\sqrt{6} \leq \beta < \alpha + \sqrt{6}$, and a repeller for $\beta < \sqrt{6}$.

2. Critical point B

At critical point B, with coordinates $x = -1$ and $y = 0$, the eigenvalues of the Jacobian matrix of the dynamical system (20) are

$$\lambda_1 = 3 + \frac{\sqrt{6}}{2}\beta \quad \text{and} \quad \lambda_2 = 3 - \frac{\sqrt{6}}{2}(\alpha - \beta), \quad (\text{A9})$$

implying that for $\beta > \alpha - \sqrt{6}$, $-\sqrt{6} < \beta < \alpha - \sqrt{6}$, and $\beta < -\sqrt{6}$ the critical point is a repeller, a saddle, and an attractor, respectively [see panel (b) of Fig. 1 and Table II].

For $\beta = \alpha - \sqrt{6}$, one of the eigenvalues, λ_2 , is zero and the other, $\lambda_1 = \sqrt{6}\alpha/2$, is positive, implying that the critical point cannot be an attractor. Let us use again the center manifold theory to determine the behavior of the orbits of the dynamical system in the vicinity of the critical point. In new variables $u = x + 1$ and $v = y$, which shift the critical point to the origin, the dynamical system (20) becomes

$$u' = f(u, v), \quad (\text{A10a})$$

$$v' = \lambda_1 v + g(u, v), \quad (\text{A10b})$$

where the nonlinear functions f and g are given by

$$f(u, v) = -3u^2 + \frac{\sqrt{6}}{2}\alpha v^2 + \frac{3}{2}u^3 - \frac{3}{2}uv^2, \quad (\text{A11})$$

$$g(u, v) = -\frac{\sqrt{6}}{2}\alpha uv + \frac{3}{2}u^2v - \frac{3}{2}v^3. \quad (\text{A12})$$

For this system, the center manifold, determined from the equation

$$\frac{dh(u)}{du}f[u, h(u)] - \lambda_1 h(u) - g[u, h(u)] = 0 \quad (\text{A13})$$

is $v = h(u) = 0$. The flow in this manifold is governed by the equation

$$u' = -3u^2 + \frac{3}{2}u^3, \quad (\text{A14})$$

from which one concludes that the critical point is a saddle node, i.e., along the u direction the orbits approach critical point B for positive u and move away from it for negative u . However, one should take into account that in coordinates u and v the phase space lies entirely on the half-plane $u \geq 0$; therefore, along the u direction all physically relevant orbits approach the critical point, while along the v direction all orbits move away from it, meaning that, from the physical point of view, the critical point can be considered a saddle. In the neighborhood of critical point B, the orbits are similar to the ones shown in panels (d), (f), and (h) of Fig. 3.

For $\beta = -\sqrt{6}$, one of the eigenvalues, λ_1 , is zero and the other, $\lambda_2 = -\sqrt{6}\alpha/2$, is negative, implying that critical point B can be either an attractor or a saddle. Let us use Lyapunov's method to show that it is an attractor.

Consider the function $V(x, y) = (x + 1)^2 + y^2$ defined on the phase space of the dynamical system (20). This function is equal to zero at critical point B and positive elsewhere. Furthermore, its derivative,

$$V' = -3(1 - x)(1 + x)^3 - 3y^4 - \frac{\sqrt{6}}{2}\alpha(1 + x)(1 - x^2 - y^2), \quad (\text{A15})$$

is negative in the neighborhood of B. Therefore, we arrive at the conclusion that the critical point is asymptotically stable and the orbits in its vicinity are similar to the ones shown in panel (i) of Fig. 3.

In summary, critical point B is a repeller for $\beta > \alpha - \sqrt{6}$, a saddle for $-\sqrt{6} < \beta \leq \alpha - \sqrt{6}$, and an attractor for $\beta \leq -\sqrt{6}$.

3. Critical point C

Critical point C, with coordinates $x = (\beta - \alpha)/\sqrt{6}$ and $y = 0$, exists for $\alpha - \sqrt{6} \leq \beta \leq \alpha + \sqrt{6}$. The corresponding eigenvalues,

$$\lambda_1 = \frac{\alpha^2 - \beta^2 + 6}{4} \quad \text{and} \quad \lambda_2 = \frac{(\alpha - \beta)^2 - 6}{4}, \quad (\text{A16})$$

imply that for $\sqrt{\alpha^2 + 6} < \beta < \alpha + \sqrt{6}$ and $\alpha - \sqrt{6} < \beta < \sqrt{\alpha^2 + 6}$ critical point C is an attractor and a saddle, respectively [see panel (c) of Fig. 1 and Table II].

For $\beta = \alpha + \sqrt{6}$, critical point C coincides with A and, therefore, the conclusions drawn above apply here, i.e., the critical point is asymptotically stable, attracting all orbits of the phase space, similarly to the situation depicted in panel (a) of Fig. 3.

For $\beta = \sqrt{\alpha^2 + 6}$, the eigenvalue λ_1 becomes zero and

$$\lambda_2 = -\frac{\alpha}{2} \left(\sqrt{\alpha^2 + 6} - \alpha \right) \quad (\text{A17})$$

is negative. To determine whether the critical point is an attractor or a saddle, let us analyze the flow on the center manifold. In variables u and v , for which the critical point is shifted to the origin, the dynamical system (20) is given by

$$u' = \lambda_2 u + f(u, v), \quad (\text{A18a})$$

$$v' = g(u, v), \quad (\text{A18b})$$

where the nonlinear functions f and g are given by

$$f(u, v) = \frac{\sqrt{6}}{2}(\sqrt{\alpha^2 + 6} - \alpha)u^2 + \frac{\sqrt{6}}{2}\alpha v^2 + \frac{3}{2}u^3 - \frac{3}{2}uv^2, \quad (\text{A19})$$

$$g(u, v) = -\frac{\sqrt{6}}{2}\alpha uv + \frac{3}{2}u^2v - \frac{3}{2}v^3. \quad (\text{A20})$$

For this system, the center manifold is approximated by the Taylor series expansion

$$u = h(v) = \frac{\sqrt{6}}{\sqrt{\alpha^2 + 6} - \alpha} v^2 + \mathcal{O}(v^4) \quad (\text{A21})$$

and the flow on it is governed by the equation

$$v' = -\frac{3}{2} \left(1 + \frac{2\alpha}{\sqrt{\alpha^2 + 6} - \alpha} \right) v^3 + \mathcal{O}(v^5). \quad (\text{A22})$$

Since the quantity in parentheses is always positive, we conclude that critical point C is an attractor for $\beta = \sqrt{\alpha^2 + 6}$. In the neighborhood of this point, the orbits are similar to the ones shown in (b) of Fig. 3.

Finally, for $\beta = \alpha - \sqrt{6}$, critical point C coincides with B and, therefore, the conclusions drawn above apply here, i.e., the critical point is a saddle and, in its neighborhood, the orbits are similar to the ones shown in panels (d), (f), and (h) of Fig. 3.

In summary, critical point C is an attractor for $\sqrt{\alpha^2 + 6} \leq \beta \leq \alpha + \sqrt{6}$ and a saddle for $\alpha - \sqrt{6} \leq \beta < \sqrt{\alpha^2 + 6}$.

4. Critical point D

Critical point D, with coordinates $x = \beta/\sqrt{6}$ and $y = \sqrt{1 - \beta^2/6}$, exists for $-\sqrt{6} \leq \beta \leq \sqrt{6}$. The eigenvalues of the Jacobian matrix of the dynamical system (20) are

$$\lambda_1 = -3 + \frac{(\alpha + \beta)\beta}{2} \quad \text{and} \quad \lambda_2 = -3 + \frac{\beta^2}{2}, \quad (\text{A23})$$

implying that for $(\sqrt{\alpha^2 + 24} - \alpha)/2 < \beta < \sqrt{6}$ and $-\sqrt{6} < \beta < (\sqrt{\alpha^2 + 24} - \alpha)/2$ the critical point is a saddle and an attractor, respectively [see panel (d) of Fig. 1 and Table II].

For $\beta = \sqrt{6}$, critical point D coincides with A and, therefore, the conclusions drawn above apply here, i.e., the critical point is a saddle and in the neighborhood of this point the orbits are similar to the ones shown in panels (b), (c), and (d) of Fig. 3.

For $\beta = (\sqrt{\alpha^2 + 24} - \alpha)/2$, the eigenvalue λ_1 becomes zero and

$$\lambda_2 = -\frac{\alpha}{4} \left(\sqrt{\alpha^2 + 24} - \alpha \right) \quad (\text{A24})$$

is negative, implying that critical point D is either an attractor or a saddle. Let us use here the central manifold theory to analyze the stability of the critical point. In the variables $u = x - \beta/\sqrt{6}$ and $v = y - \sqrt{1 - \beta^2/6}$, which shift the critical point to the origin, the dynamical system (20) becomes

$$u' = \sqrt{\frac{3}{2}\alpha^2 - \lambda_2^2} v + f(u, v), \quad (\text{A25a})$$

$$v' = \lambda_2 v + g(u, v), \quad (\text{A25b})$$

where the nonlinear functions f and g are given by

$$f(u, v) = \frac{\sqrt{6}}{4} \sqrt{\alpha^2 + 24} u^2 - 3 \sqrt{1 - \frac{2\lambda_2^2}{3\alpha^2}} uv + \frac{\sqrt{6}}{4} \alpha v^2 + \frac{3}{2} u^3 - \frac{3}{2} uv^2, \quad (\text{A26})$$

$$g(u, v) = \frac{3}{2} \sqrt{1 - \frac{2\lambda_2^2}{3\alpha^2}} u^2 - \frac{9}{2} \sqrt{1 - \frac{2\lambda_2^2}{3\alpha^2}} v^2 + \frac{3}{2} u^2 v - \frac{3}{2} v^3. \quad (\text{A27})$$

In order to apply the center manifold theorem, the differential equation for the variable u should not contain linear terms. Therefore, we perform a new change of variables,

$$w = u + v \sqrt{\frac{3\alpha^2}{2\lambda_2^2} - 1} \quad \text{and} \quad z = v, \quad (\text{A28})$$

that brings the dynamical system (A25) to the required form, namely,

$$w' = F(w, z), \quad (\text{A29a})$$

$$z' = \lambda_2 z + G(w, z), \quad (\text{A29b})$$

where the nonlinear functions F and G are given by

$$F(w, z) = -\frac{3\sqrt{6}\alpha}{2\lambda_2} w^2 + \sqrt{\frac{3}{-\lambda_2}} (3\lambda_2 - \alpha^2) wz - \frac{\sqrt{6}\alpha}{4\lambda_2} (\alpha^2 - 2\lambda_2) z^2 + \frac{3}{2} w^3 - \frac{3\alpha}{\sqrt{-2\lambda_2}} w^2 z - \frac{3}{4\lambda_2} (2\lambda_2 + \alpha^2) w z^2, \quad (\text{A30})$$

$$G(w, z) = \frac{\sqrt{-3\lambda_2}}{2} w^2 - \frac{\sqrt{6}\alpha}{2} w z + \frac{1}{4} \sqrt{\frac{3}{-\lambda_2}} (6\lambda_2 + \alpha^2) z^2 + \frac{3}{2} w^2 z - \frac{3\alpha}{\sqrt{-2\lambda_2}} w z^2 - \frac{3}{4\lambda_2} (\alpha^2 + 2\lambda_2) z^3. \quad (\text{A31})$$

In these new variables, the center manifold is given by

$$z = h(w) = \sqrt{\frac{3}{\alpha(\sqrt{\alpha^2 + 24} - \alpha)}} w^2 + \mathcal{O}(w^3) \quad (\text{A32})$$

and the flow on it is determined by

$$w' = \frac{6\sqrt{6}}{\sqrt{\alpha^2 + 24} - \alpha} w^2 + \mathcal{O}(w^3). \quad (\text{A33})$$

From the above equation, we conclude that along the w direction the orbits approach critical point D for negative w and move away from it for positive w , meaning that D is a saddle node. However, one should take into account that in coordinates w and z the phase space is the upper part of an ellipse lying entirely on the half-plane $w \leq 0$; therefore, all physically relevant orbits approach

critical point D, which is then, from this point of view, an attractor. In the neighborhood of this point, the orbits are similar to the ones shown in panels (g) and (h) of Fig. 3.

For $\beta = -\sqrt{6}$, critical point D coincides with B and, therefore, the conclusions drawn above apply here, i.e., the critical point is asymptotically stable, attracting all the orbits of the phase space, similarly to the situation depicted in panel (i) of Fig. 3.

In summary, critical point D is a saddle for $(\sqrt{\alpha^2 + 24} - \alpha)/2 < \beta \leq \sqrt{6}$ and an attractor for $-\sqrt{6} \leq \beta \leq (\sqrt{\alpha^2 + 24} - \alpha)/2$.

5. Critical point E

Critical point E, with coordinates $x = \sqrt{6}/(\alpha + \beta)$ and $y = \sqrt{6 + \alpha^2 - \beta^2}/(\alpha + \beta)$, exists for $(\sqrt{\alpha^2 + 24} - \alpha)/2 \leq \beta \leq \sqrt{\alpha^2 + 6}$. The eigenvalues of the Jacobian matrix of the dynamical system (20) are

$$\lambda_{1,2} = -\frac{3\alpha}{2(\alpha + \beta)} \left(1 \pm \sqrt{1 + K} \right), \quad (\text{A34})$$

where

$$K = \frac{2(\beta^2 + \alpha\beta - 6)(\beta^2 - \alpha^2 - 6)}{3\alpha^2}. \quad (\text{A35})$$

For $(\sqrt{\alpha^2 + 24} - \alpha)/2 < \beta < \sqrt{\alpha^2 + 6}$, K is negative and, therefore, the real parts of the eigenvalues λ_1 and λ_2 are also negative, implying that point E is an attractor [see panel (e) of Fig. 1 and Table II]. If $-1 \leq K < 0$, the attractor is a node; if $K < -1$, it is a spiral. Since the former condition corresponds to two thin regions of the parameter space adjacent to the curves $\beta = \sqrt{\alpha^2 + 6}$ and $\beta = (\sqrt{\alpha^2 + 24} - \alpha)/2$, in most cases critical point E is a spiral attractor, as shown in panels (c), (d), (e), and (f) of Fig. 3.

For $\beta = \sqrt{\alpha^2 + 6}$, critical point E coincides with C and, therefore, the conclusions drawn above apply here, i.e., the critical point is an attractor and, in its neighborhood, the orbits are similar to the ones shown in panel (b) of Fig. 3.

Finally, for $\beta = (\sqrt{\alpha^2 + 24} - \alpha)/2$, critical point E coincides with D and, thus, all physically relevant orbits approach it. In the neighborhood of this point, the orbits are similar to the ones shown in panels (g) and (h) of Fig. 3.

In summary, whenever critical point E exists, it is an attractor.

-
- [1] A. G. Riess *et al.* (Supernova Search Team), Observational evidence from supernovae for an accelerating universe and a cosmological constant, *Astron. J.* **116**, 1009 (1998).
- [2] S. Perlmutter *et al.* (Supernova Cosmology Project), Measurements of Ω and Λ from 42 high-redshift supernovae, *Astrophys. J.* **517**, 565 (1999).
- [3] P. A. R. Ade *et al.* (Planck Collaboration), Planck 2015 results: XIII. Cosmological parameters, *Astron. Astrophys.* **594**, A13 (2016).
- [4] S. Weinberg, The cosmological constant problem, *Rev. Mod. Phys.* **61**, 1 (1989).
- [5] J. Martin, Everything you always wanted to know about the cosmological constant problem (but were afraid to ask), *C. R. Phys.* **13**, 566 (2012).
- [6] E. J. Copeland, M. Sami, and S. Tsujikawa, Dynamics of dark energy, *Int. J. Mod. Phys. D* **15**, 1753 (2006).
- [7] G. Bertone and T. M. P. Tait, A new era in the search for dark matter, *Nature (London)* **562**, 51 (2018).
- [8] S. Capozziello, S. Nojiri, and S. D. Odintsov, Unified phantom cosmology: Inflation, dark energy and dark matter under the same standard, *Phys. Lett. B* **632**, 597 (2006).
- [9] A. R. Liddle, C. Pahud, and L. A. Ureña-López, Triple unification of inflation, dark matter, and dark energy using a single field, *Phys. Rev. D* **77**, 121301(R) (2008).
- [10] N. Bose and A. S. Majumdar, k-essence model of inflation, dark matter, and dark energy, *Phys. Rev. D* **79**, 103517 (2009).
- [11] A. B. Henriques, R. Potting, and P. M. Sá, Unification of inflation, dark energy, and dark matter within the Salam-Sezgin cosmological model, *Phys. Rev. D* **79**, 103522 (2009).
- [12] J. De-Santiago and J. L. Cervantes-Cota, Generalizing a unified model of dark matter, dark energy, and inflation with a noncanonical kinetic term, *Phys. Rev. D* **83**, 063502 (2011).
- [13] S. D. Odintsov and V. K. Oikonomou, Unification of inflation with dark energy in $f(R)$ gravity and axion dark matter, *Phys. Rev. D* **99**, 104070 (2019).
- [14] G. B. F. Lima and R. O. Ramos, Unified early and late Universe cosmology through dissipative effects in steep quintessential inflation potential models, *Phys. Rev. D* **100**, 123529 (2019).
- [15] P. M. Sá, Triple unification of inflation, dark energy, and dark matter in two-scalar-field cosmology, *Phys. Rev. D* **102**, 103519 (2020).
- [16] A. Arbey and J.-F. Coupechoux, Unifying dark matter, dark energy and inflation with a fuzzy dark fluid, *J. Cosmol. Astropart. Phys.* 01 (2021) 033.
- [17] V. K. Oikonomou, Unifying inflation with early and late dark energy epochs in axion $F(R)$ gravity, *Phys. Rev. D* **103**, 044036 (2021).
- [18] A. L. Berkin and K. I. Maeda, Inflation in generalized Einstein theories, *Phys. Rev. D* **44**, 1691 (1991).
- [19] A. A. Starobinsky, S. Tsujikawa, and J. Yokoyama, Cosmological perturbations from multi-field inflation in generalized Einstein theories, *Nucl. Phys.* **B610**, 383 (2001).

- [20] T. Harko, T. S. Koivisto, F. S. N. Lobo, and G. J. Olmo, Metric-Palatini gravity unifying local constraints and late-time cosmic acceleration, *Phys. Rev. D* **85**, 084016 (2012).
- [21] N. Tamanini and C. G. Böhrer, Generalized hybrid metric-Palatini gravity, *Phys. Rev. D* **87**, 084031 (2013).
- [22] P. M. Sá, Unified description of dark energy and dark matter within the generalized hybrid metric-Palatini theory of gravity, *Universe* **6**, 78 (2020).
- [23] L. Amendola, Scaling solutions in general nonminimal coupling theories, *Phys. Rev. D* **60**, 043501 (1999).
- [24] D. J. Holden and D. Wands, Self-similar cosmological solutions with nonminimally coupled scalar field, *Phys. Rev. D* **61**, 043506 (2000).
- [25] A. P. Billyard and A. A. Coley, Interactions in scalar field cosmology, *Phys. Rev. D* **61**, 083503 (2000).
- [26] L. Amendola, Coupled quintessence, *Phys. Rev. D* **62**, 043511 (2000).
- [27] D. Tocchini-Valentini and L. Amendola, Stationary dark energy with a baryon-dominated era: Solving the coincidence problem with a linear coupling, *Phys. Rev. D* **65**, 063508 (2002).
- [28] B. Gumjudpai, T. Naskar, M. Sami, and S. Tsujikawa, Coupled dark energy: towards a general description of the dynamics, *J. Cosmol. Astropart. Phys.* 06 (2005) 007.
- [29] C. G. Böhrer, G. Caldera-Cabral, R. Lazkoz, and R. Maartens, Dynamics of dark energy with a coupling to dark matter, *Phys. Rev. D* **78**, 023505 (2008).
- [30] K. Tzanni and J. Miritzis, Coupled quintessence with double exponential potentials, *Phys. Rev. D* **89**, 103540 (2014).
- [31] S. Singh and P. Singh, It's a dark, dark world: background evolution of interacting ϕ CDM models beyond simple exponential potentials, *J. Cosmol. Astropart. Phys.* 05 (2016) 017.
- [32] F. F. Bernardi and R. G. Landim, Coupled quintessence and the impossibility of an interaction: a dynamical analysis study, *Eur. Phys. J. C* **77**, 290 (2017).
- [33] Yu. L. Bolotin, A. Kostenko, O. A. Lemets, and D. A. Yerokhin, Cosmological evolution with interaction between dark energy and dark matter, *Int. J. Mod. Phys. D* **24**, 1530007 (2015).
- [34] B. Wang, E. Abdalla, F. Atrio-Barandela, and D. Pavón, Dark matter and dark energy interactions: theoretical challenges, cosmological implications and observational signatures, *Rep. Prog. Phys.* **79**, 096901 (2016).
- [35] S. Bahamonde, C. G. Böhrer, S. Carloni, E. J. Copeland, W. Fang, and N. Tamanini, Dynamical systems applied to cosmology: Dark energy and modified gravity, *Phys. Rep.* **775-777**, 1 (2018).
- [36] E. J. Copeland, A. R. Liddle, and D. Wands, Exponential potentials and cosmological scaling solutions, *Phys. Rev. D* **57**, 4686 (1998).
- [37] C. Wetterich, Cosmology and the fate of dilatation symmetry, *Nucl. Phys.* **B302**, 668 (1988).
- [38] J. Carr, *Applications of Centre Manifold Theory* (Springer, New York, 1982).
- [39] J. Guckenheimer and P. Holmes, *Nonlinear Oscillations, Dynamical Systems, and Bifurcations of Vector Fields* (Springer, New York, 1983).
- [40] O. I. Bogoyavlensky, *Methods in the Qualitative Theory of Dynamical Systems in Astrophysics and Gas Dynamics* (Springer-Verlag, Berlin, Heidelberg, 1985).